NASA TECHNICAL NOTE

NASA TN D-6678

MAXIMUM POWER TRANSFER FROM A SOLAR-CELL ARRAY BY SENSING ARRAY TEMPERATURE

by Merton Sussman

Langley Research Center
Hampton, Va. 23365

NATIONAL AERONAUTICS AND SPACE ADMINISTRATION • WASHINGTON, D. C. • MARCH 1972

1. Report No.	2. Government Accession No.	3. Recipient's Catalog No.
NASA TN D-6678		

4. Title and Subtitle	5. Report Date
MAXIMUM POWER TRANSFER FROM A SOLAR-CELL ARRAY BY SENSING ARRAY TEMPERATURE	March 1972
	6. Performing Organization Code

7. Author(s)	8. Performing Organization Report No.
Merton Sussman	L-8110
	10. Work Unit No.
9. Performing Organization Name and Address	113-34-22-01
NASA Langley Research Center Hampton, Va. 23365	11. Contract or Grant No.
	13. Type of Report and Period Covered
12. Sponsoring Agency Name and Address	Technical Note
National Aeronautics and Space Administration Washington, D.C. 20546	14. Sponsoring Agency Code

15. Supplementary Notes

16. Abstract

A technique is described in which a spacecraft solar-cell array is caused to operate at or near maximum power output over a wide range of environmental conditions. The output of an array temperature sensor is used to vary the duty cycle of a pulse-width-modulated impedance regulator so that the array operates at the voltage of maximum power. A resistance-type temperature sensor was found to be applicable for most spacecraft missions. However, a solar cell used as a temperature sensor has the advantage of negligible transient errors on lightweight arrays for orbiting spacecraft.

17. Key Words (Suggested by Author(s))	18. Distribution Statement
Maximum power transfer from solar-cell array Impedance matching Power conditioning Temperature sensing dc transformer	Unclassified – Unlimited

19. Security Classif. (of this report)	20. Security Classif. (of this page)	21. No. of Pages	22. Price*
Unclassified	Unclassified	39	$3.00

*For sale by the National Technical Information Service, Springfield, Virginia 22151

MAXIMUM POWER TRANSFER FROM A SOLAR-CELL ARRAY BY SENSING ARRAY TEMPERATURE

By Merton Sussman
Langley Research Center

SUMMARY

This report describes a method in which a solar-cell array is caused to operate at or near maximum power output over a wide range of environmental conditions. The method is based on controlling the operating load impedance of the solar-cell array. Array temperature is sensed and converted into a control signal. The conditioned control signal alters the input impedance of a pulse-width-modulated regulator as a function of array temperature; thereby, the array is permitted to operate at or near maximum power output.

Two array temperature sensors and associated signal conditioning networks were investigated. A resistance-type temperature sensor was found to be generally applicable on spacecraft missions where rapid array temperature excursions are not anticipated, such as space probes. One or more solar cells used as a temperature sensor may be applicable for orbital missions unless relatively wide variations in illumination and/or irradiation are anticipated.

INTRODUCTION

Solar-cell arrays are generally used to supply electrical power on most of the spacecraft that have a mission lifetime greater than a few days. Since solar arrays are relatively large and expensive, it is important to utilize the maximum power available. The optimum array load for maximum utilization of power is a function of array temperature. Generally, an array designed for minimum weight normally experiences wide temperature extremes. Optimum loading of an array is also dependent on the illumination intensity, which, in turn, is dependent upon the attitude of the array with respect to the sun and its distance from the sun. Optimum loading is also affected by array degradation caused by the radiation environment.

The array output voltage at maximum power is primarily a function of array temperature and is only slightly affected by changes in illumination level and moderate radiation damage. The approach to realization of maximum power discussed in this paper

utilizes the output of an array temperature sensor to vary the duty cycle of a state-of-the-art pulse-width-modulated impedance regulator so that the array operates at its voltage of maximum power.

SYMBOLS

C	capacitors, subscripts denoting different circuit locations
D	free-wheeling diode
d	duty cycle factor of the pulse-width-modulated regulator, dimensionless
I_c	capacitor charging current of the pulse-width-modulator, amperes dc
I_i	input current to the pulse-width-modulated regulator, amperes dc
I_o	output current of the pulse-width-modulated regulator, amperes dc
K_1, K_2, K_4, K_6, K_8	sensitivity factors
K_3, K_5, K_7, K_9	dc level constants
L	filter choke
m	change in array voltage at maximum power with change in array temperature over approximately linear high-temperature range, volts/^oC
Q	transistors, subscripts denoting different circuit locations
R	resistor, subscripts denoting different circuit locations
R_i	reflected input resistance of pulse-width-modulated regulator, ohms
R_o	effective load resistance of the pulse-width-modulated regulator, ohms
R_s	resistance of array temperature sensor, ohms
T	solar-cell array temperature, ^oC

t	time, seconds
V_A	solar-cell array voltage, volts dc
V_B	battery voltage, volts dc
$V_{b,1}$	array temperature-sensitive voltage between base and ground of pulse-width-modulated control transistor, volts dc
$V_{b,3}$	array temperature-sensitive voltage between base and ground of solar-cell sensor dc amplifier, volts dc
$V_{b,3A}$	component of $V_{b,3}$ corresponding to a shorted regulated supply, volts dc
$V_{b,3B}$	component of $V_{b,3}$ corresponding to a shorted solar-cell sensor, volts dc
V_C	solar-cell array temperature sensor voltage, volts dc
V_{ce}	collector-to-emitter voltage of switching power transistor, volts dc
V_i	input voltage to the pulse-width-modulated regulator, volts dc
V_o	output voltage of the pulse-width-modulated regulator, volts dc
V_p	solar-cell array voltage at maximum power, volts dc
V_{po}	solar-cell array voltage at maximum power for a certain chosen array temperature, volts dc
V_s	regulated supply voltage for pulse-width-modulator and solar-cell sensor dc amplifier, volts dc
V_{sc}	solar-cell sensor voltage, volts dc
v_d	instantaneous voltage across free-wheeling diode, volts
τ	constant switching period for switching power transistor, seconds

Subscripts:

off	part of switching period for which switching power transistor is nonconducting
on	part of switching period for which switching power transistor is conducting
sat	saturated condition

FACTORS AFFECTING ARRAY MAXIMUM POWER

Figure 1 shows the variation of array current and power with array voltage for a typical solar-cell array at several temperatures. Illumination level is assumed to be constant, and the temperature extremes shown are typical of those experienced by the conservatively designed Lunar Orbiter spacecraft array. At the highest temperature shown, 100° C, a maximum of 170 watts is available at an array voltage of 29.4 volts. When the array temperature is -100° C, 380 watts are available at 67 volts. In many spacecraft power systems the array is directly coupled to a rechargeable battery, as shown in the simplified schematic diagram of figure 2. In such a system the array is constrained to operate at the battery charging voltage. Usually, the array is designed so that the battery-charging voltage is near the maximum power voltage of the array at the highest expected array temperature. Therefore, most of the extra power available at colder temperatures is not utilized. To utilize the maximum power generated at all array temperatures, a variable-impedance matching circuit is needed which will allow the array to operate at maximum power. The power generated at a voltage that is a function of temperature is thus converted into dc power at a relatively constant voltage.

The solar-cell data presented in this paper are based on using typical N on P, 10 ohm-cm silicon solar cells. However, the described method of obtaining maximum power is not restricted to this particular type of solar cell.

Figure 3 further indicates the advantage of obtaining maximum power from a typical array on a planetary or lunar orbiter. The array temperature drops rapidly during orbital darkness and can reach very low values if the effective thermal mass is low, or if the orbital dark period is long. The maximum power available from the array during orbital sunlight is shown compared with the power utilized if the array is directly coupled to the battery. Batteries of the nickel-cadmium type normally used for this purpose have a relatively constant charging voltage. They can accept very high charging rates when partially discharged, but as the fully charged level is approached, the charging rate must be considerably reduced. Therefore, by tracking maximum array power, the extra power available at low array temperatures can be effectively used to charge the battery.

Figure 4 illustrates the need for obtaining maximum power from a solar-cell array on a spacecraft that was proposed to orbit the sun. (See ref. 1.) Approximate expected mission parameter values were an array temperature of 85° C, predicted at perihelion (approximately 0.60 astronomical unit (AU) from the sun), and an array temperature of 6° C at aphelion (1.0 AU). (1 AU is defined as the mean distance from the earth to the sun, 149 599 000 km.) At perihelion, 36 watts is shown to be available at the maximum power point, but power output would drop rapidly above the maximum power voltage of 13 volts. At aphelion, 18 watts is shown to be available at the maximum power point, but only 12 watts would be utilized if the array voltage is held at 13 volts. A similar problem exists on other space missions whenever an appreciable variation in the distance between the spacecraft and the sun is expected.

In figure 5, curves of maximum power and voltage at maximum power with temperature are given for a typical 1- by 2-cm solar cell. A curve of open-circuit voltage is also shown for comparison. The two curves of voltage plotted against temperature are similar in shape, the voltage at maximum power being roughly 90 millivolts less than that for an open circuit. These curves are usually linear at the high temperatures but deviate slightly from linearity at the low temperatures.

Figure 6 shows typical curves of solar-cell current plotted against voltage supplied by a solar-cell manufacturer for various illumination levels but with cell temperature held constant. The curves are normalized to the solar-cell curve at 1 astronomical unit. It should be noted that over the range of illumination levels from approximately 30 to 500 mW/cm^2, the voltage at maximum power does not vary more than ± 3 percent. A curve for current plotted against voltage typical of solar cells that have experienced approximately 22-percent power degradation because of simulated space radiation (ref. 2) is also shown in figure 6. Again, the voltage at maximum power is not drastically changed. Figures 7 and 8 show that the effect on solar-cell voltage at maximum power due to a variation of illumination and due to radiation damage, respectively, is reasonably constant over a wide range of solar-cell temperatures. The data in figure 7 were collected at the Langley Research Center by Gilbert A. Haynes, and the data in figure 8 were obtained from reference 3. Hence, even over a wide range of illumination levels as long as the array is not subjected to heavy radiation damage, only array temperature needs to be sensed to obtain voltage at maximum power.

DESIGN PHILOSOPHY

The pulse-width-modulated type of impedance regulator was selected for use in this study because it can be designed to be very efficient and relatively reliable. As indicated in the simplified block diagram of figure 9, a small dc signal V_C controls the

fractional on-time, or duty cycle factor, of the series-connected transistor switch. The basic circuit is often used as a conventional voltage regulator (ref. 4) and, for this purpose, the control signal is the deviation of output voltage from a fixed reference voltage. With appropriate input and output filtering, the circuit can be considered as a dc transformer where the duty cycle factor d is analogous to a turns ratio. Hence, if no losses are assumed, the averaged input voltage V_i, current I_i, and resistance R_i are related to the averaged output voltage V_o, current I_o, and resistance R_o by the following relations:

$$d = \frac{V_o}{V_i} = \frac{I_i}{I_o} = \sqrt{\frac{R_o}{R_i}} \tag{1}$$

Appendix A gives the derivation of the equation

$$d = \frac{V_o}{V_i}$$

A solar-cell array can be automatically matched to its loads to obtain maximum power by supplying a control signal to the pulse-width modulator of figure 9 that is an appropriate function of the voltage at maximum power. The approach used in this investigation is to obtain the control signal from an array temperature sensor. A suitable signal-conditioning network modifies the sensor output voltage so that the optimum ratio of battery voltage to array voltage is automatically maintained.

The technique of obtaining maximum power can be described mathematically. In equation (1) the input and output regulator voltages are, respectively, the solar-array voltage and the battery voltage. Therefore,

$$d = \frac{V_B}{V_A} \tag{2}$$

It is desired for the array to operate at the voltage of maximum power V_p. Consequently,

$$d = \frac{V_B}{V_p} \tag{3}$$

It is true that the battery-charging voltage V_B is not a constant; however, it varies over a narrow range. For example, for a nominal 28-volt system, the charging voltage of a nickel-cadmium battery would typically vary from about 30.0 volts to 32.5 volts.

The array voltage at maximum power with array temperature is very close to being a linear characteristic, particularly for array temperatures above approximately 0° C. Therefore, it can be assumed that

$$V_p = -mT + V_{po} \tag{4}$$

Substituting equation (4) into equation (3) yields

$$d = \frac{V_B}{-mT + V_{po}} \tag{5}$$

Note that in order for the array to operate at the voltage of maximum power, the power-system duty cycle must vary inversely with the solar-array temperature.

The array does not have to operate at the voltage of maximum power precisely in order to utilize the array maximum power effectively. In figure 10, values of relative array power plotted against normalized array voltage operating error at several array temperatures are given. Array power compared with array voltage is relatively broad in the vicinity of the maximum power point. At the worst conditions of -119° C, if the array voltage is maintained to within ± 5 percent of that at maximum power, the array operates within approximately 95 percent of maximum power. Since the array voltage at maximum power does not have to be realized to a high degree of accuracy, the sensing and signal-conditioning circuitry can be relatively simple and consist of only a few components.

The pulse-width-modulated regulator of figure 9 can only reduce array voltage; hence, the solar array should be designed so that its voltage at maximum power, at the highest expected array operating temperature, is slightly above the battery voltage. By designing a buck-boost type of regulator, array voltage could be boosted, but at the expense of both efficiency and reliability. In the configuration shown, a shorted switching transistor is not catastrophic since the array is then directly coupled to the battery and loads. However, an open-switching transistor would result in total loss of array power.

Several variations of the basic concept illustrated in figure 9 have been proposed that allow a solar-cell array to operate near maximum power. (See refs. 5 to 9.) In each of these approaches, relatively complex circuitry and a cyclic variation in the operating point of the solar array are used to derive the signal that controls pulse width. In the approach discussed in reference 5, the ac or dynamic impedance of the array is measured and used to derive the control signal. In the techniques proposed in references 6 and 7, the derivative of array power with time during the cyclic variations is determined and used in a closed-loop circuit to control pulse width automatically and to maximize the power transferred from the array. Somewhat similar techniques are employed in reference 8 to maximize battery charge current and in reference 9 to maximize power delivered to the battery.

When compared with the other techniques proposed for obtaining maximum array power, the control circuitry required for the approach discussed in this paper is consid-

erably less complex. It is basically an open-loop system and hence requires that critical components be compensated for circuit-temperature variations and component aging.

SOLAR-CELL-ARRAY TEMPERATURE-SENSING CIRCUITS

Resistive-Type Temperature Sensor

Figure 11 is a schematic diagram showing details of the control and sensing circuitry and the pulse-width modulator of the system indicated in figure 9. The resistive temperature sensor R_S with resistors R_3, R_1, and R_2 form a voltage divider circuit. The latter two resistors represent the signal conditioning network, which is designed to produce the desired characteristic of duty cycle factor with array temperature. Appendix B shows how R_S and the signal-conditioning network are determined. Resistors R_3, R_4, and R_5 provide bias, some degree of circuit temperature stabilization, and base current limiting, respectively.

The pulse-width modulator consists of transistors Q_1 and Q_2, capacitor C, and the level detector. Array temperature determines the value of R_S which controls the base current of Q_1, which, in turn, controls the charging current of capacitor C. The charging rate of the capacitor determines the time during a switching period that the level detector initiates an output voltage. This voltage is maintained until the capacitor is discharged through Q_2. Hence, a series of pulses, whose duty cycle factor depends upon array temperature, is generated at the fixed frequency of the pulse generator. These pulses, after amplification, periodically turn off the switching power transistor of the circuit in figure 9. The loss of control signal will thus result in a continuous "on" condition or a duty cycle factor of 100 percent.

It can be explained mathematically how the variation of duty cycle factor with array temperature of the pulse-width modulator can be made to satisfy the desired relationship of equation (5). The duty cycle factor of the modulator varies inversely with capacitor charging current

$$d = \frac{K_1}{I_c} \tag{6}$$

The capacitor-charging current varies linearly with the base to ground voltage of Q_1, but with a negative slope

$$I_c = -K_2 V_{b,1} + K_3 \tag{7}$$

If the sensor resistance is linear with temperature and has a positive temperature coefficient, the base to ground voltage of Q_1 is

$$V_{b,1} = K_4 T + K_5 \tag{8}$$

Substituting equation (8) into equation (7) results in

$$I_c = -K_6T + K_7 \tag{9}$$

Substituting equation (9) into equation (6) results in

$$d = \frac{K_1}{-K_6T + K_7} \tag{10}$$

Note from equation (10) that the duty cycle of the pulse-width modulator varies inversely with array temperature. Furthermore, equation (10) has the same form as that of equation (5). These two facts are the basis for the choice of this particular pulse-width-modulator circuit for this investigation. The purpose of the signal-conditioning network is to adjust the value of the constants $(K_1$ to $K_7)$ of the modulator so that the array voltage operating error is minimized.

In the circuit of figure 11, a fixed-pulse generator frequency of 10 kHz was chosen for this investigation as a compromise between system efficiency and filter component weight. A generator pulse width of 12 microseconds was found to be compatible with the required duty cycle range of 40 to 100 percent.

Several types of thin low-mass sensors, designed for surface-temperature measurements, are available and suitable for array-temperature measurements. Those utilizing fine platinum wire, with a positive temperature coefficient of 0.0039 (ohms/ohm)/^{o}C, have the best long-term stability. Nickel sensors, with a temperature coefficient of 0.0067 (ohms/ohm)/^{o}C, should be satisfactory for many applications. Semiconductor-type sensors are available with higher coefficients, but their calibrations may change when subjected to space radiation. Conventionally designed temperature sensors should be satisfactory for measuring array temperatures on deep space probes where temperature changes are gradual, or on orbiting spacecraft where the thermal mass of the array is conservatively designed. However, to minimize temperature errors on lightweight arrays, sensor-mounting techniques and thermal-control coatings should be chosen with care. To minimize thermal transient errors on orbiting spacecraft having solar cells bonded to very lightweight substrates, the sensor should be designed and mounted to simulate closely the thermal characteristics of the solar cells.

Solar Cell Used as a Temperature Sensor

Since the output voltage of a solar cell is a function of temperature, a solar cell can be used as a temperature sensor. Figures 12 and 13 show the variation of the solar-cell sensor characteristics with array temperature for various fixed values of sensor-load resistance. As can be seen in figure 13, adjusting the value of the solar-cell sensor load resistance varies the shape of the curve of sensor voltage plotted against array tempera-

ture. The specific value of sensor load resistance is not very critical. The typical load resistance range is 12 to 22 ohms for 1- by 2-cm cells. A lower value of load resistance could be used if it is desirable to limit battery charge currents at very low temperatures. A sensor cell of the same type as the cells used on the array to generate power, and mounted in the same manner, should have negligible thermal transient errors even on very lightweight spacecraft arrays.

A solar-cell temperature sensor can be used to best advantage on very lightweight solar-oriented arrays on orbiting spacecraft. It must be continuously illuminated during the sunlit part of the orbit and is not accurate if subjected to either appreciable radiation or variations in illumination. (See fig. 6.)

Figure 14 is a schematic diagram showing details of the control and sensing circuitry built for use with a solar-cell temperature sensor in the pulse-width-modulated regulator of figure 9. The only difference between this circuit and the one shown in figure 11 is the signal conditioning network, consisting of the transistor dc amplifying stage Q_3 and resistors R_A to R_I. The solar-cell sensor load resistor R_A is small compared with R_B and is trimmed to obtain the desired shape of the curve for the array voltage at maximum power as a function of array temperature. Resistors R_B, R_C, and R_D are determined to produce the system sensitivity and dc level that results in the desired characteristic of duty cycle as a function of array temperature. Resistors R_G, R_H, and R_I form a biasing network for Q_1. Appendix C outlines the procedure used to determine the values of resistors R_A, R_B, R_C, and R_D. For reliability reasons, the circuit of figure 14 is designed so that one terminal of the solar cell could be grounded. An alternate approach is one that utilizes several sensor solar cells connected in series to eliminate the need for the dc amplifying stage Q_3.

PERFORMANCE TESTS

Test Setup

Figure 15 is a block diagram of the test setup used in the laboratory investigation of the maximum power concept. The sub-setup (A) was used with the resistive-type temperature sensor and sub-setup (B) was used with the solar-cell temperature sensor. A solar-cell array simulator, shown in figure 16, was used to simulate an array consisting of 10 parallel-connected strings of 100 series-connected solar cells per string. Test data were obtained for a simulated oriented array on a spacecraft in a planetary orbit. The array temperature range of -120° C to 100° C was simulated by varying the number of silicon diodes used in the simulator. The simulated array temperature varies inversely with the number of silicon diodes used. The array illumination intensity was simulated at a value of 140 mW/cm^2 by operating the current power supply at an appropriate constant value of current. The battery simulator of figure 15 is a shunt voltage

regulator adjusted to simulate the charging characteristics of a 20-cell, 3-ampere-hour nickel-cadmium battery.

Discussion of Results

The curves shown in figures 17 and 18 are representative of data obtained by utilizing a solar cell as a temperature sensor. Data obtained by utilizing a resistive-type temperature sensor are very similar.

Figure 17 shows that the largest array voltage operating error, over the array temperature range of -120° C to 100° C, is -4.15 volts. This error is equivalent to an array voltage operating percentage error of -10.4 percent. Figure 17 also shows the variation of the sum of battery and load current. The load current remained approximately constant at 345 mA; hence, the variation of battery current tapered from a maximum of 880 mA at the lowest array temperature indicated to a minimum of 200 mA at the highest array temperature. The salient feature of figure 17 is that the regulator converts dc power at approximately constant current and at a voltage that varies with temperature into dc power at an essentially constant voltage, the current varying with temperature.

Figure 18 shows a comparison between the maximum available array power and the array power obtained over the indicated temperature range. At an array temperature of approximately 65° C, 94.7 percent of the maximum available array power is obtained. This percentage is the worst array power utilization and corresponds to the largest array voltage operating error of -10.4 percent. These results were obtained with a solar-cell sensor load resistance of 22 ohms. By changing the value of sensor load resistance and readjusting the various signal conditioning parameters, it is possible to reduce the operating error. Since the pulse-width-modulated impedance regulator does have some losses, the power at the output of the regulator is less than the array power obtained. During the laboratory tests, it was determined that the regulator efficiency varied from 93 to 85 percent which corresponded to an array temperature range of from 92.6° C to -120° C, respectively. It is possible to improve the regulator efficiency by optimizing the circuit for the particular mission under consideration. Areas for improvement might include choosing the optimum switching power transistor, designing the optimum filter, and reducing standby power losses.

Figure 18 also compares the output power from the regulator with the array power that would be obtained if the array were directly coupled to the battery and load. If the curve of temperature plotted against time of figure 3 is assumed, the total equivalent energy after the switching regulator is 21 watt-hours, whereas only 18 watt-hours are available from the solar array if it is directly coupled to the battery and load. This value is equivalent to an energy improvement factor of 16.7 percent. The advantage of obtaining maximum array power becomes greater as the array temperature extremes become wider.

CONCLUDING REMARKS

The technique described will cause a spacecraft solar-cell array to operate at, or very closely to, its maximum power point over a wide range of environmental conditions. It was shown that on a typical orbiting solar-oriented spacecraft which experiences a sunlight interval of 60 minutes and array-temperature extremes of approximately $\pm 100^{\circ}$ C, the array could deliver approximately 95 percent or more of the maximum power available when this technique is used. This technique resulted in an increase of 16.7 percent in energy utilized to recharge the battery.

Two types of array-temperature sensors and their associated signal conditioning networks were investigated. A resistance-type temperature sensor is generally applicable for most spacecraft missions. However, a solar cell used as a temperature sensor has the advantage of negligible transient errors on lightweight arrays for orbiting spacecraft.

Langley Research Center,
National Aeronautics and Space Administration,
Hampton, Va., February 4, 1972.

APPENDIX A

DERIVATION OF $d = \frac{V_o}{V_i}$

The purpose of this appendix is to show that the ratio of dc output voltage to the dc input voltage of a pulse-width-modulating regulator is equal to the duty cycle of the regulator. Therefore, the following equation is to be derived:

$$d = \frac{V_o}{V_i} \tag{A1}$$

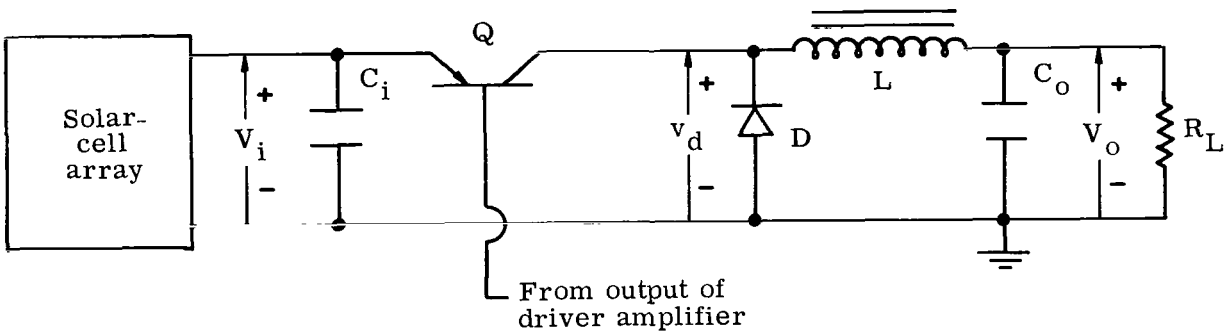

Sketch (a).- Pulse-width-modulator switching regulator power system.

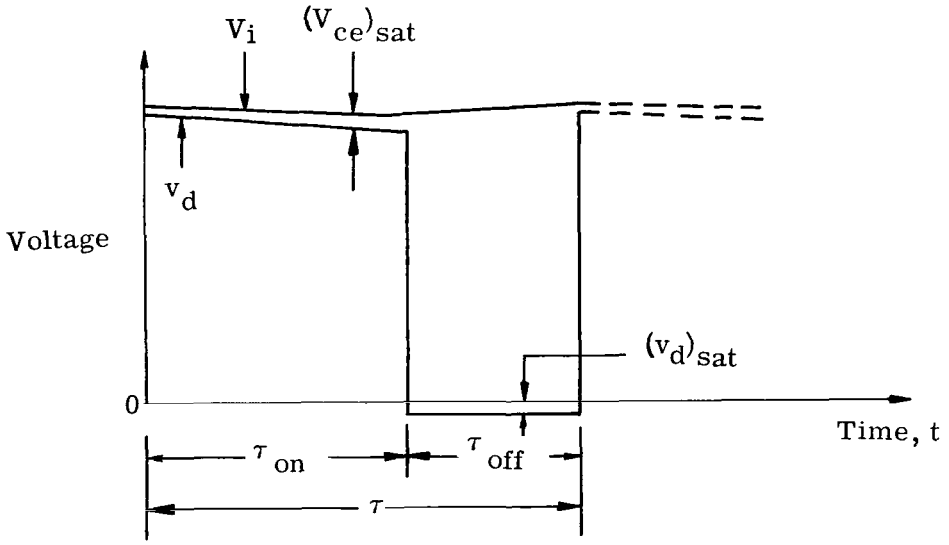

Sketch (b).- Typical waveforms of solar-array voltage and diode voltage.

The dc resistance of the filter choke L shown in sketch (a) is generally very low; therefore, its value can be assumed to be zero. By referring to sketches (a) and (b)

$$V_o = \frac{1}{\tau}\int_0^{\tau} v_d \, dt \tag{A2}$$

$$V_o = \frac{1}{\tau}\left(\int_0^{\tau_{on}} v_d \, dt + \int_{\tau_{on}}^{\tau} v_d \, dt\right) \tag{A3}$$

For $0 \leqq t \leqq \tau_{on}$,

$$v_d = V_i - (V_{ce})_{sat} \tag{A4}$$

For $\tau_{on} \leqq t \leqq \tau$,

$$v_d = (v_d)_{sat} \tag{A5}$$

For a high-quality switching power transistor Q and a high-quality switching power diode D, the saturated collector to emitter voltage and saturated diode voltage, respectively, are each so small that their values can be assumed to be negligible compared with the output voltage from a conventional array. Also, it is assumed the power transistor and power diode switch instantaneously. Therefore, the rise time and fall time are each assumed to be zero. Hence,

$$V_o = \frac{1}{\tau}\left(\int_0^{\tau_{on}} V_i \, dt + \int_{\tau_{on}}^{\tau} (0) \, dt\right) \tag{A6}$$

For a properly chosen input filter capacitor C_i, V_i will essentially remain constant during $0 \leqq t \leqq \tau_{on}$. Hence,

$$V_o = \frac{V_i}{\tau}\int_0^{\tau_{on}} dt = \frac{V_i}{\tau}\tau_{on} \tag{A7}$$

$$\frac{V_o}{V_i} = \frac{\tau_{on}}{\tau} \tag{A8}$$

Let the definition of duty cycle factor be

$$d = \frac{\tau_{on}}{\tau} \tag{A9}$$

Consequently,

$$d = \frac{V_o}{V_i} \tag{A10}$$

APPENDIX B

DESIGNING THE RESISTIVE TEMPERATURE SENSOR AND SIGNAL-CONDITIONING NETWORK TO OBTAIN MAXIMUM ARRAY POWER

The purpose of this appendix is to describe the criteria used for determining the values of resistance for resistors R_S, R_1, and R_2 of figure 11. The control circuit shown in sketch (c) can be used to determine the values of R_V which simulates the resistive network consisting of R_S, R_1, and R_2 in figure 11. For convenience, R_V can be a resistive decade box. The test procedure consists of manually adjusting the

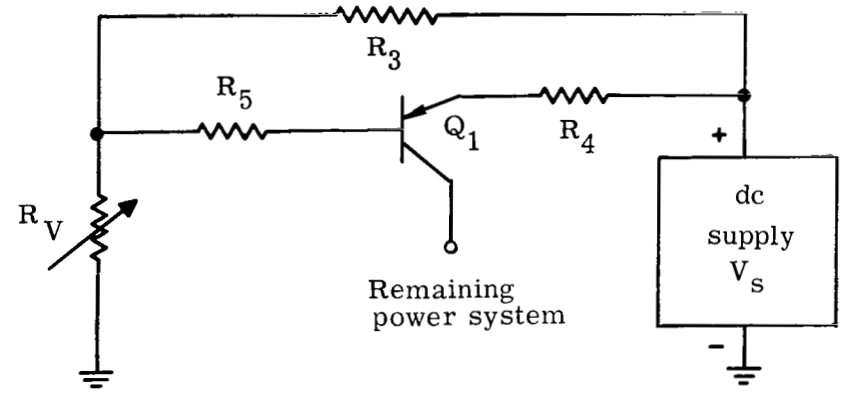

Sketch (c).- Test setup for determining values or R_S, R_1, and R_2.

value of R_V so that for each simulated array temperature, the array voltage is equal to the value at maximum power. Although it is not shown in sketch (c), it should be understood that the entire power system is used for this test.

In general, there will not be a resistive temperature-sensing element that follows the required characteristic of R_V as a function of array temperature with sufficient accuracy. It will usually be necessary to modify the characteristic of the sensor for resistance with temperature so that it approximates closer the required characteristic. This modification can be accomplished by connecting resistors in series and in parallel with the resistive temperature-sensing element, as is shown in figure 11. It can be seen that

$$R_V = \frac{(R_S + R_1)R_2}{R_S + R_1 + R_2} \tag{B1}$$

The specific resistive temperature-sensing element R_S can be chosen on the basis of the required characteristic of R_V as a function of temperature. The next step in the process is to choose judiciously two simulated array temperatures and to determine the values of R_V and R_S at these two temperatures. The values for R_S and R_V at these two temperatures are substituted into equation (B1); as a result, there are two equations (one equation for each temperature) and two unknowns $(R_1$ and $R_2)$. The unknowns R_1 and R_2 can then be solved by the method of simultaneous equations. A special point should be made of the fact that the sensitivity of the resistance with temperature of the chosen R_S has to be greater than the corresponding required value since the action of R_1 and R_2 is to reduce the effective overall sensitivity.

APPENDIX C

DESIGNING THE SOLAR-CELL TEMPERATURE SENSOR AND SIGNAL-CONDITIONING NETWORK TO OBTAIN MAXIMUM ARRAY POWER

The purpose of this appendix is to describe the criteria used for determining the values of resistance for resistors R_A, R_B, R_C, and R_D of figure 14. The first step is to determine the required base-to-ground voltage of Q_3 with array temperature so that for each simulated array temperature, the array operates at the voltage of maximum power. This information is obtained by using the test control circuit of sketch (d). Although not shown in this sketch, it should be understood that the entire power system is used for this test. Let it be assumed that the values for resistors R_E to R_J have

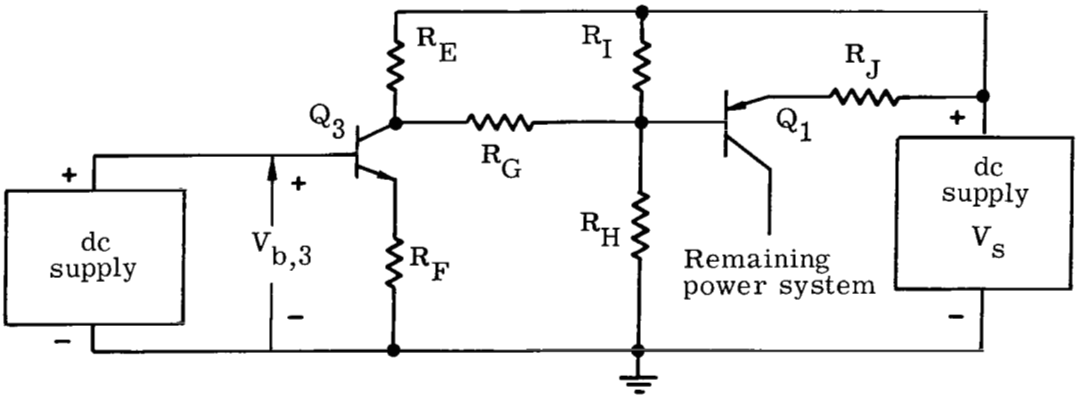

Sketch (d).- Test setup for determining required variation of $V_{b,3}$ with array temperature.

been determined by basic standard transistor circuitry calculations. The next step is to determine values for R_B, R_C, and R_D. Sketch (e) aids in determining these resistive values. Again, the entire power system is used for this test. An equation of $V_{b,3}$ in terms of V_{sc}, V_s, R_B, R_C, and R_D can be derived. Let $R_C \ll R_D$ so that the effective base-to-ground resistance of the Q_3 stage remains essentially constant.

By using the principle of linear superposition with the V_s supply shorted,

$$V_{b,3A} = \frac{R_C}{R_B + R_C} V_{sc} \tag{C1}$$

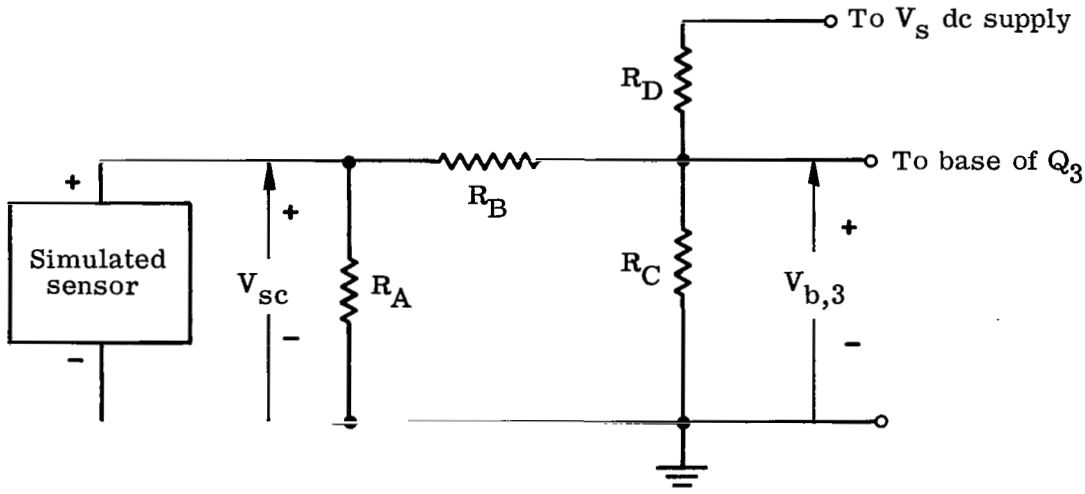

Sketch (e).- Analysis of required R_B, R_C, and R_D.

(This equation is valid since $R_C \ll R_D$). With the V_{sc} sensor shorted,

$$V_{b,3B} = \frac{\frac{R_B R_C}{R_B + R_C}}{\frac{R_B R_C}{R_B + R_C} + R_D} V_s \tag{C2}$$

and

$$V_{b,3} = V_{b,3A} + V_{b,3B} \tag{C3}$$

Hence, $V_{b,3}$ as a function of V_{sc}, R_B, R_C, R_D, and V_s is shown in the following equation:

$$V_{b,3} = \frac{R_C}{R_B + R_C} V_{sc} + \frac{R_B R_C V_s}{R_B R_C + R_B R_D + R_C R_D} \tag{C4}$$

Equation (C4) is the working equation. The constant V_s represents the supply voltage of the dc power supply. The required curve for $V_{b,3}$ against array temperature is known from the test described by sketch (d). The curve obtained for V_{sc} as a function of array temperature is known since the solar-cell sensor and its load have been chosen. The quantity R_B is chosen to be a relatively low value; for example, R_B = 5000 ohms would be a good typical value. Equation (C4) can be used to solve for R_C and R_D by

the method of simultaneous equations. This solution is made by choosing two array temperatures and relating these temperatures to the corresponding $V_{b,3}$ and V_{sc} values. By assigning a value to R_B, R_C and R_D can be determined.

Note that equation (C4) is of the form

$$Y = K_8X + K_9 \tag{C5}$$

The sensitivity K_8 and the operating bias K_9 of the dc amplifier stage of Q_3 are modified by adjusting the values of R_B, R_C, and R_D.

REFERENCES

1. Anon.: The Conceptual Design of a Small Solar Probe (Sunblazer). MIT CSR TR-69-1 (Contract No. NASr-249), Massachusetts Inst. Technol., Jan. 1969. (Available as NASA CR-100034.)

2. Haynes, Gilbert A.; and Ellis, Walter E.: Effects of 22 MeV Proton and 2.4 MeV Electron Radiation on Boron- and Aluminum-Doped Silicon Solar Cells. NASA TN D-4407, 1968.

3. Martin, J. H.; Teener, J. W.; and Ralph, E. L.: Some Effects of Electron Irradiation and Temperature on Solar Cell Performance. Proceedings 17th Annual Power Sources Conference, U.S. Army Electron. Res. Develop. Lab., May 1963, pp. 15-19.

4. Hnatek, Eugene R.: Design of Solid-State Power Supplies. Van Nostrand Reinhold Co., c.1971, pp. 189-204.

5. Paulkovich, John: Slope Detection as a Method of Determining the Peak Power Point of Solar Arrays. X-636-64-282, NASA Goddard Space Flight Center, 1964. (Available as NASA TM X-55137.)

6. Knauer, Paul: Automatic Impedance Matching in DC Circuits. IEEE Aerosp. & Electron. Syst. Conv. Record, vol. AES-2, no. 6, Nov. 1966, pp. 38-42.

7. Hartman, David A.: Adaptive Power Conditioning for Solar Cell Arrays. IEEE Aerosp. & Electron. Syst. Conv. Record, vol. AES-2, no. 6, Nov. 1966, pp. 43-47.

8. Anon.: Nondissipative Solar Array Optimum Charge Regulator. Rep. No. P66-181 (Contract No. NAS 5-9210), Aerospace Group, Hughes Aircraft Co., July 1966. (Available as NASA CR-79093.)

9. Gladstone, B.; and Yuh, J.: Final Report for Optimum Charging System Study Program Rep. No. 1906 (Contract No. NAS 5-3785), Engineered Magnetics Div., Gulton Industries, Inc., Aug. 1, 1966. (Available as NASA CR-81367.)

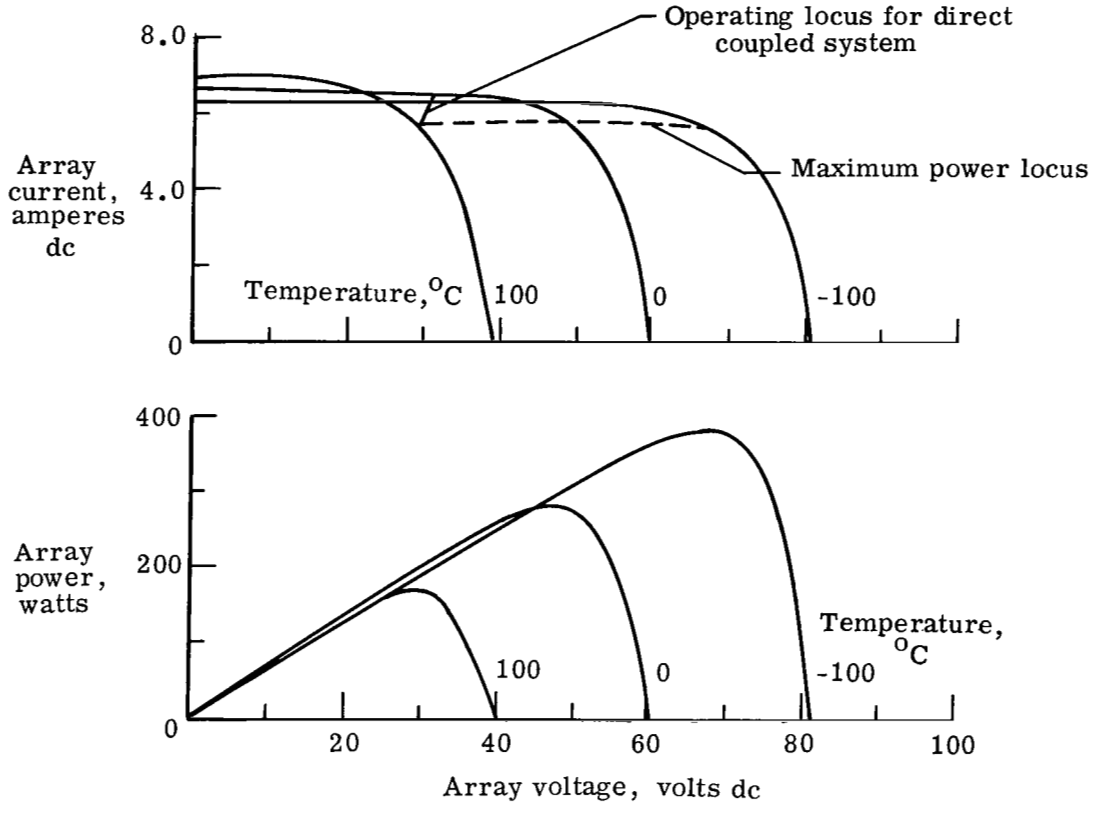

Figure 1.- Solar-cell array characteristics for a lunar or planetary orbiting spacecraft. Illumination intensity, 140 mW/cm^2.

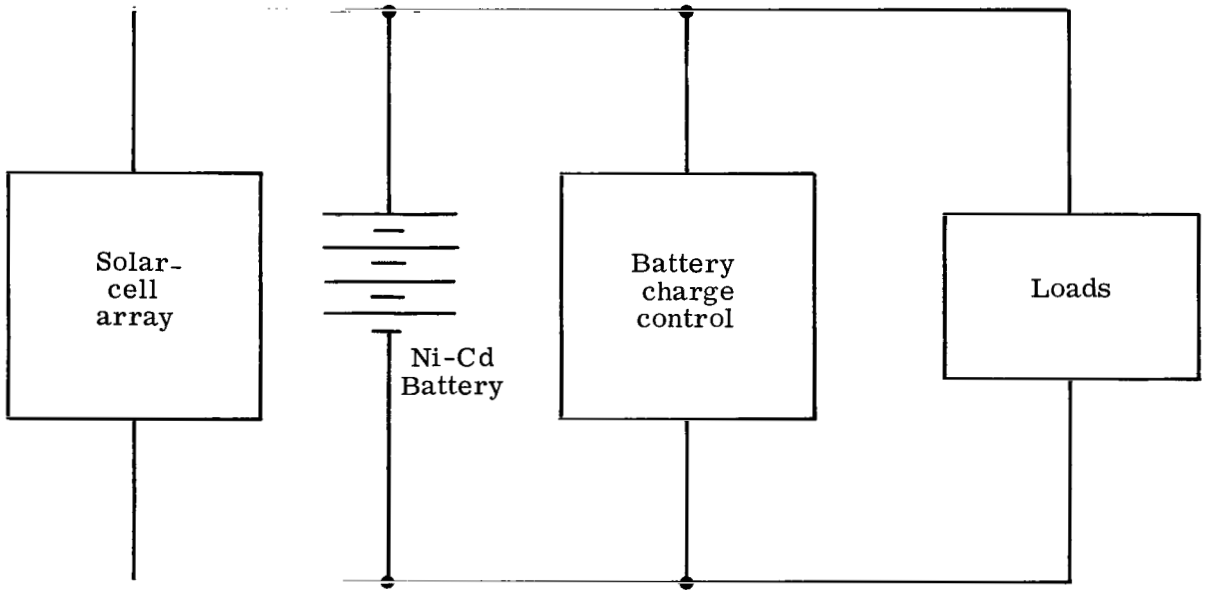

Figure 2.- Block diagram of a typical directly coupled solar-cell array spacecraft power system.

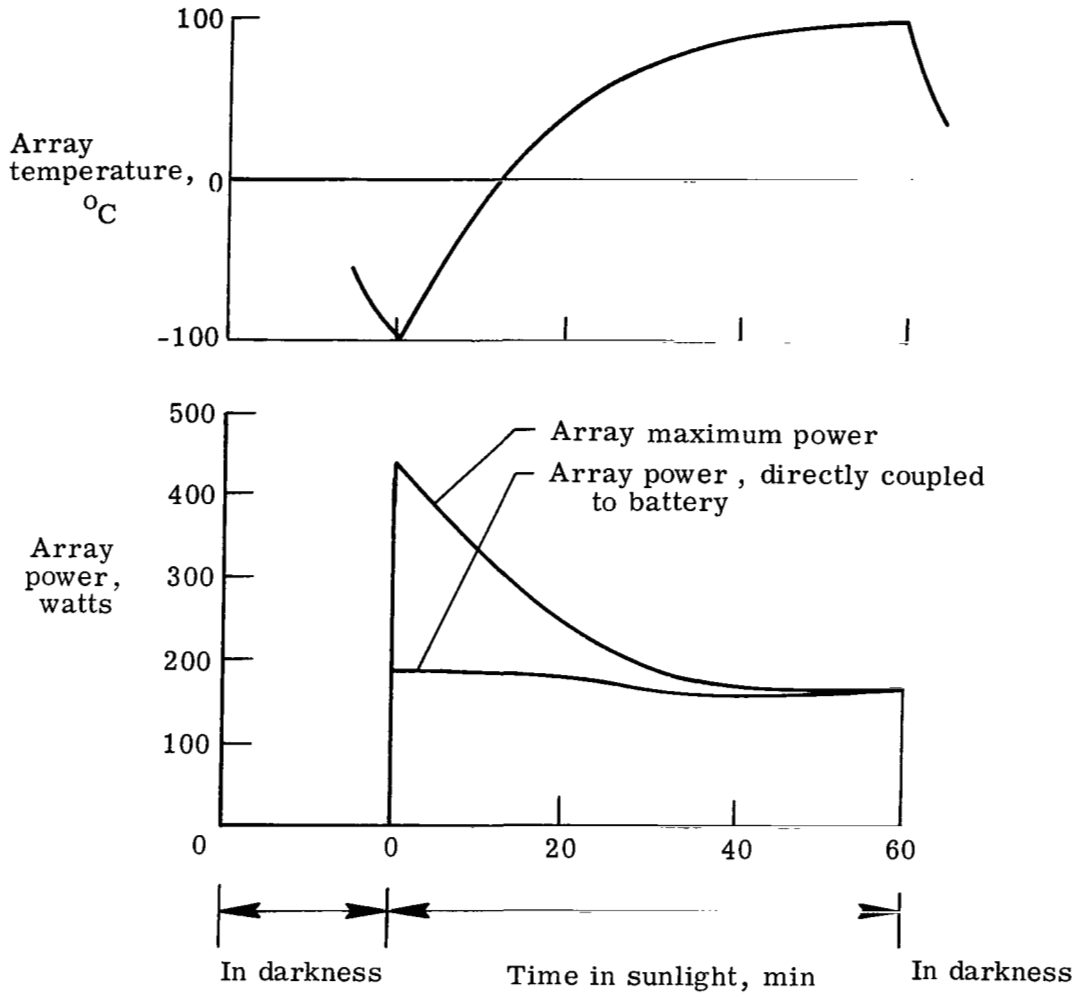

Figure 3.- Variation of temperature and power with time in orbit for a solar-cell array. Illumination intensity, 140 mW/cm^2.

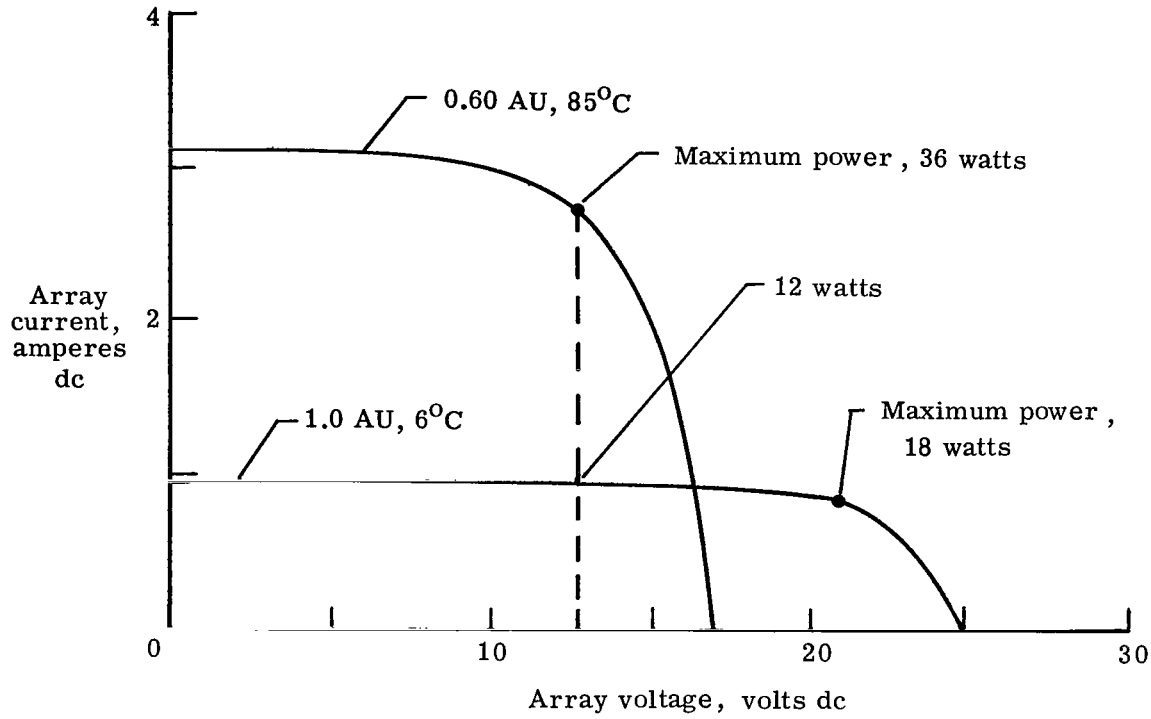

Figure 4.- Solar-cell array characteristics on a solar orbiting spacecraft.

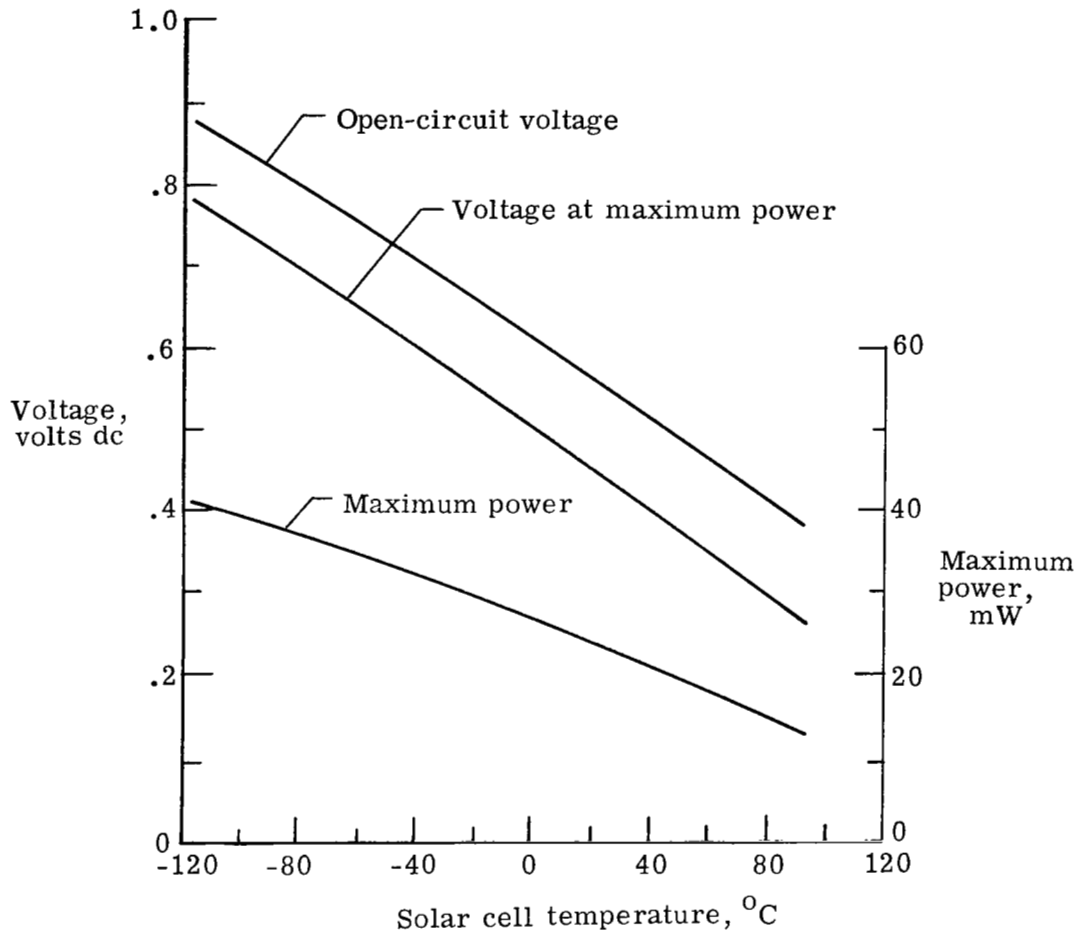

Figure 5.- Variation of solar-cell voltage at maximum power, open-circuit voltage, and maximum power with temperature. Illumination intensity, 140 mW/cm^2.

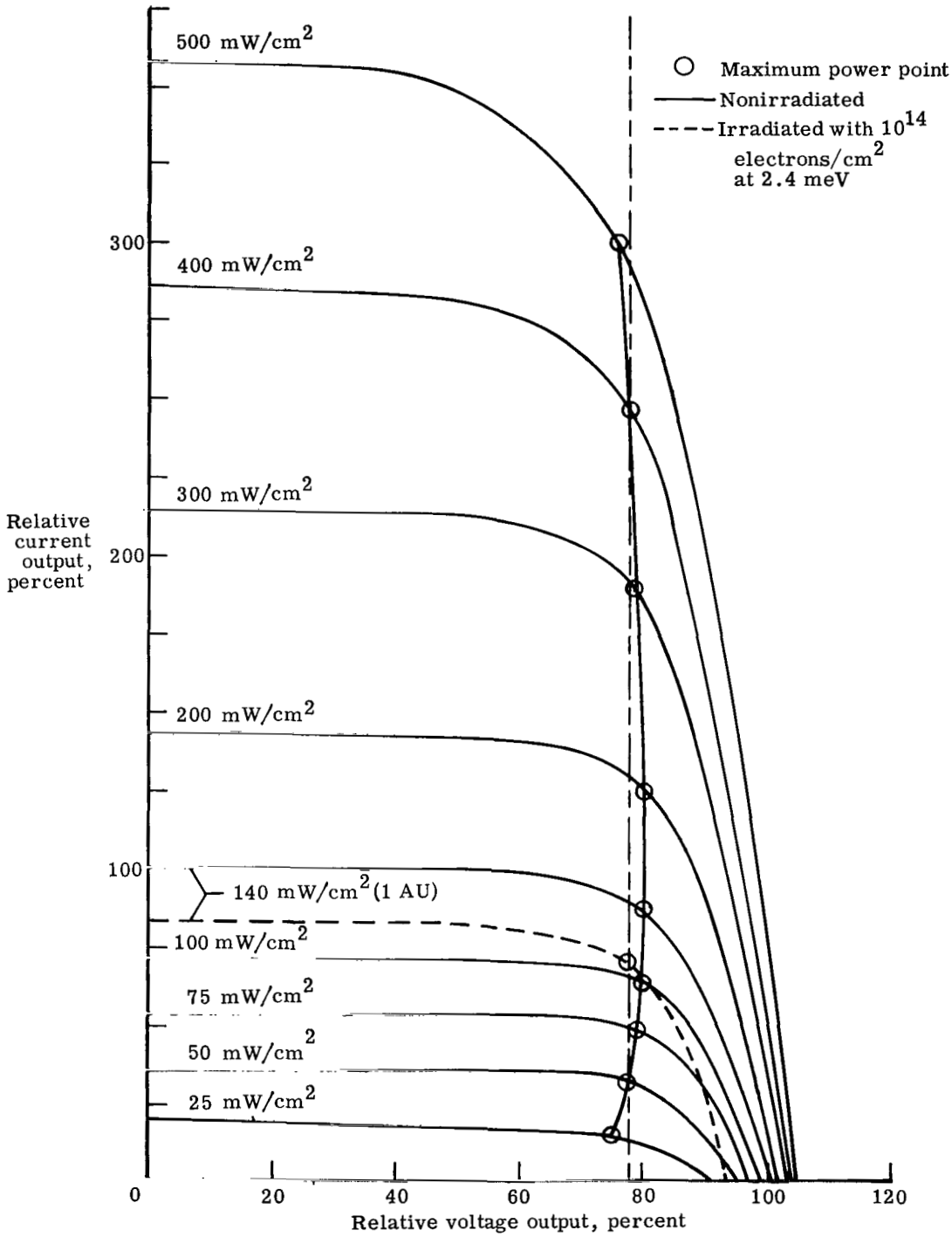

Figure 6.- The effects of solar-cell illumination intensity and irradiation on the voltage at maximum power.

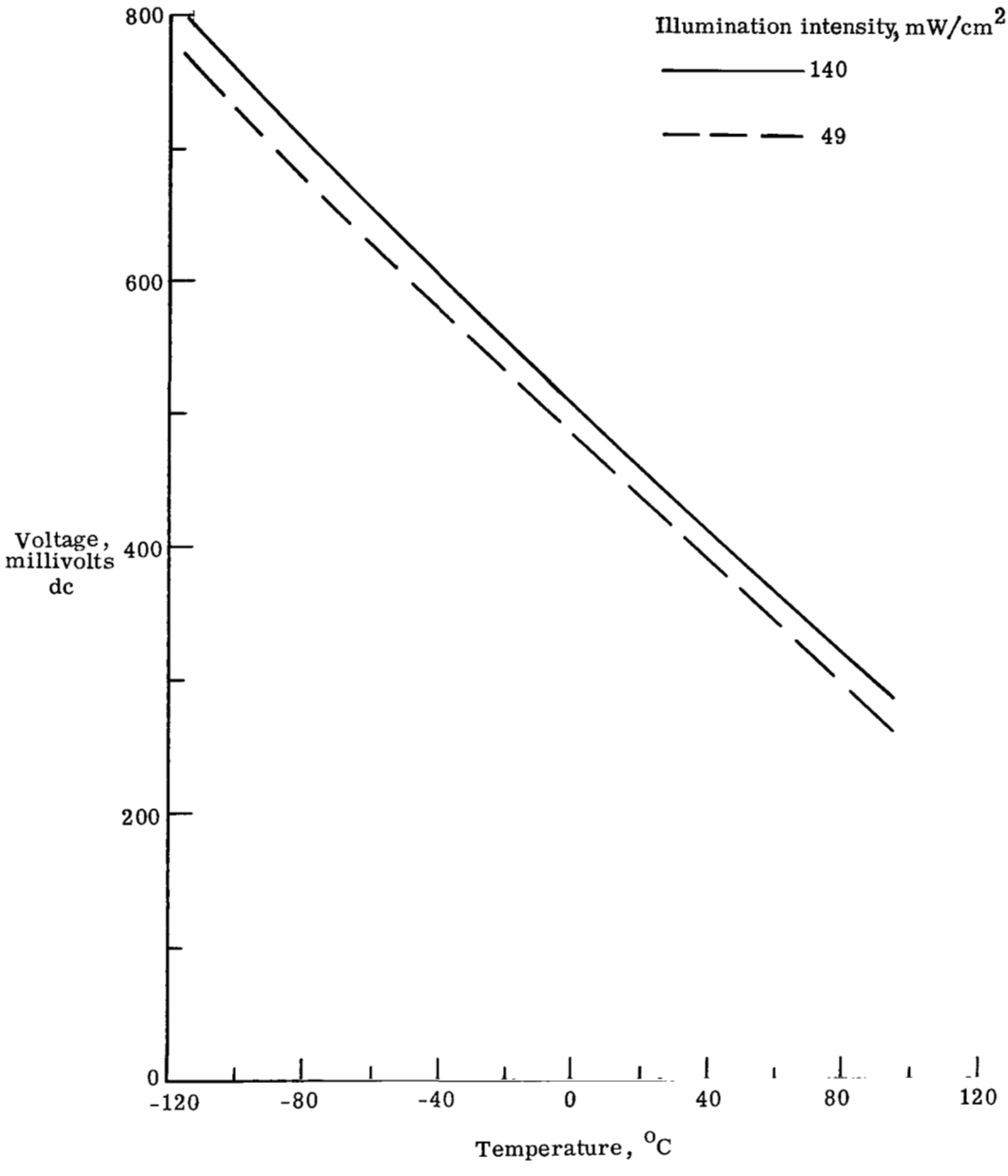

Figure 7.- Variation of voltage at maximum power with temperature of a typical solar cell at two levels of illumination intensity.

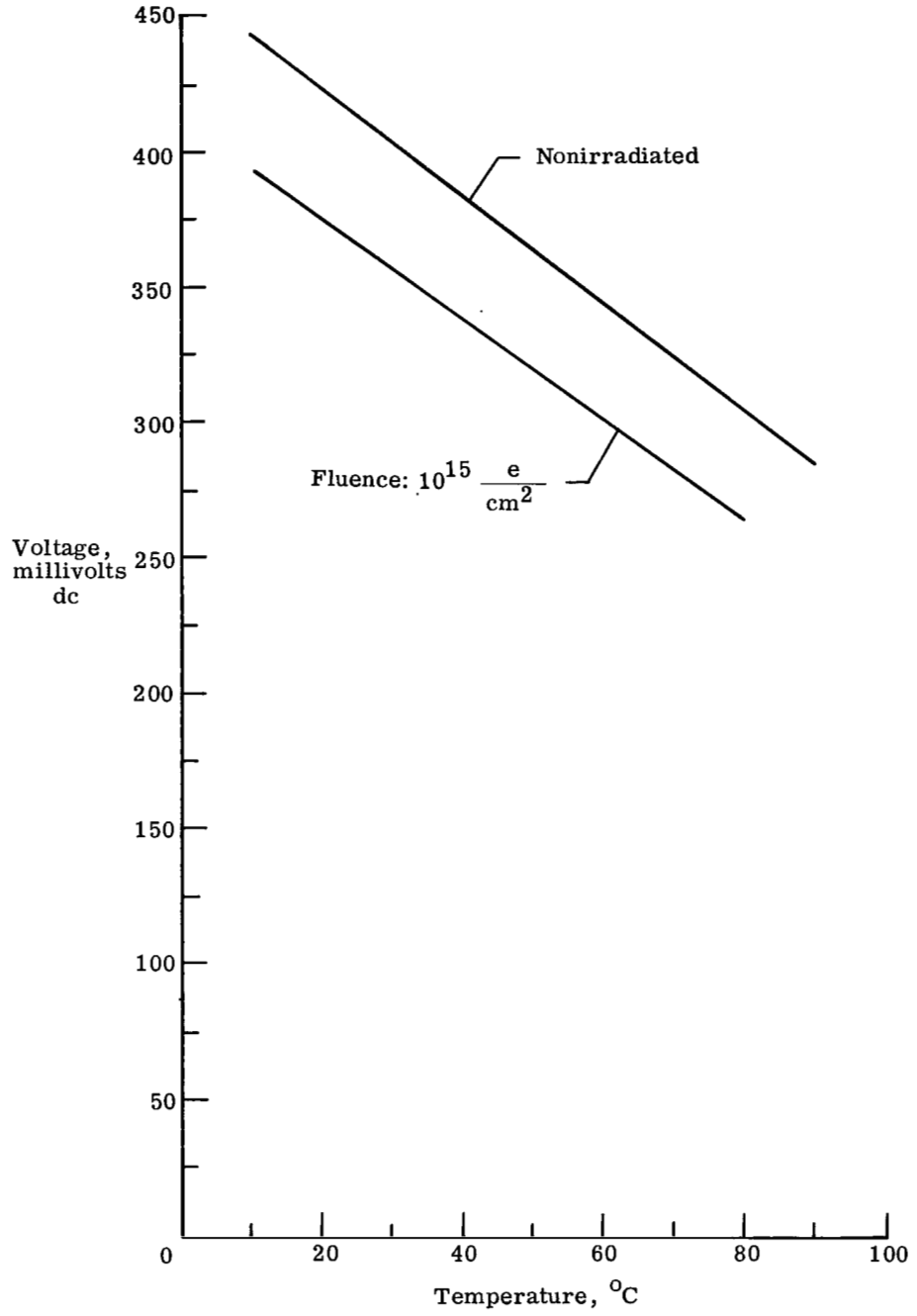

Figure 8.- The effect of 1 MeV electron radiation on the voltage at maximum power for a typical solar cell. Illumination intensity, 140 mW/cm^2.

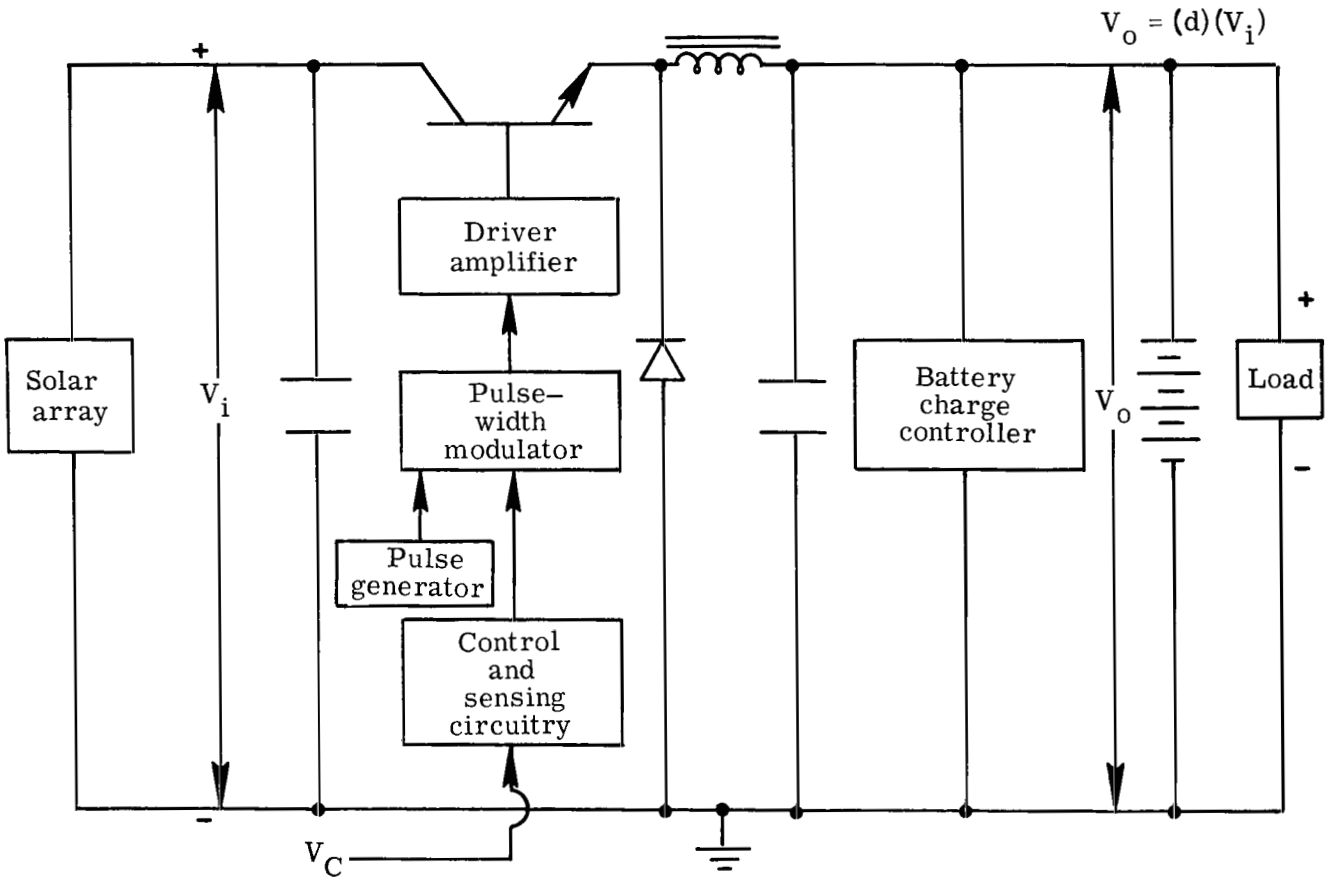

Figure 9.- Block diagram of a power system using a pulse-width-modulated impedance regulator.

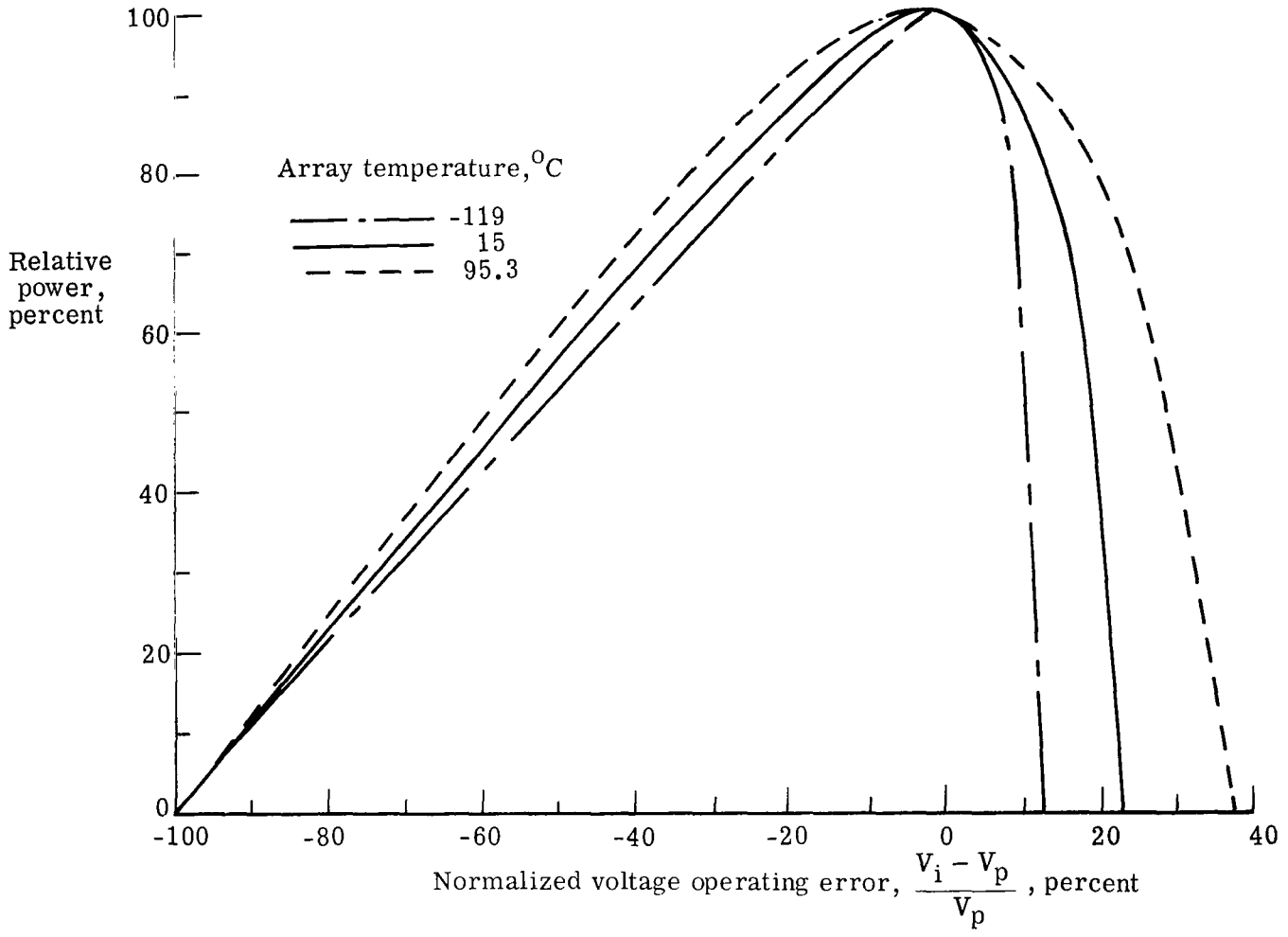

Figure 10.- Variation of relative array power with normalized array voltage operating error. Illumination intensity, 140 mW/cm2.

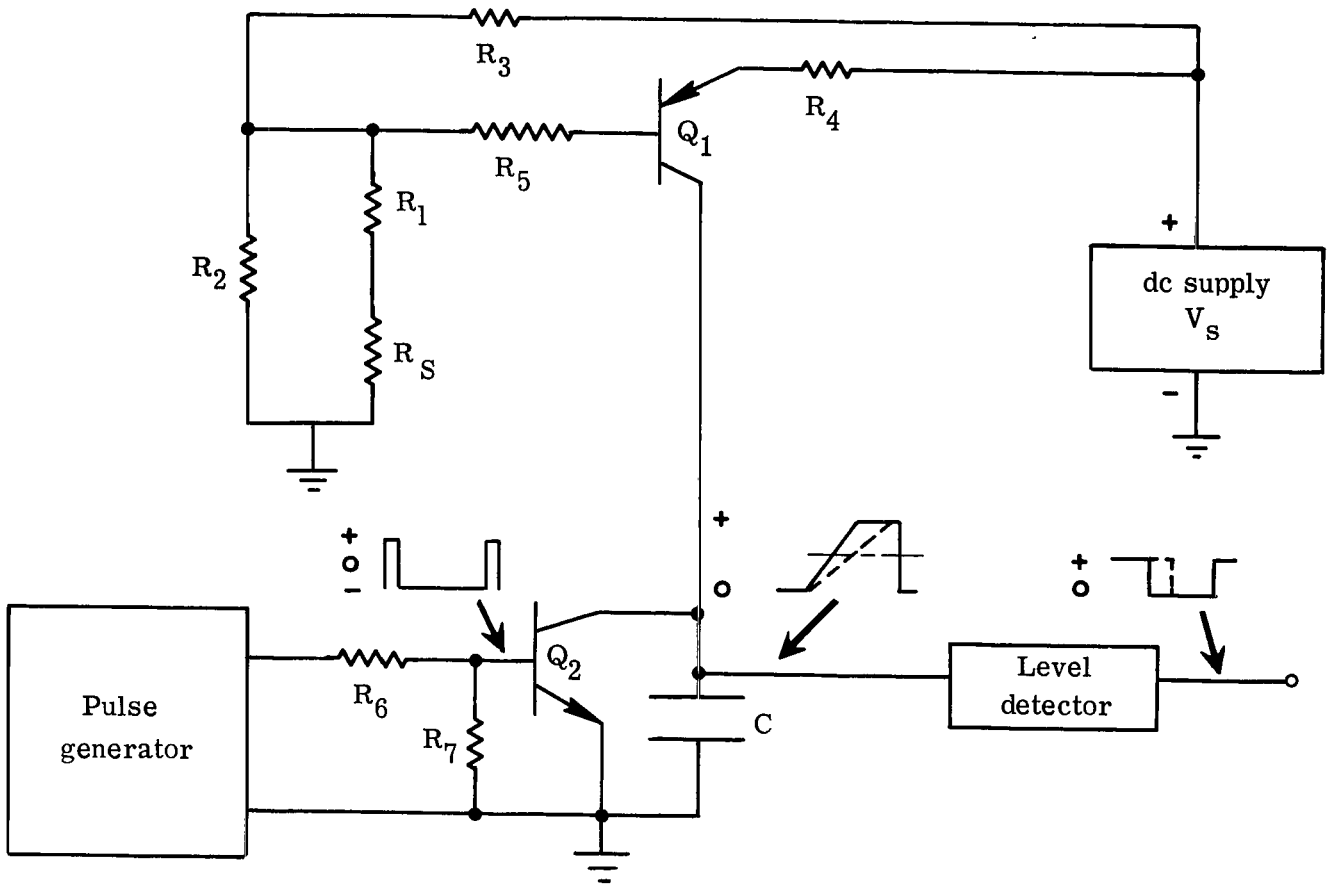

Figure 11.- Control circuit utilizing resistive temperature sensor.

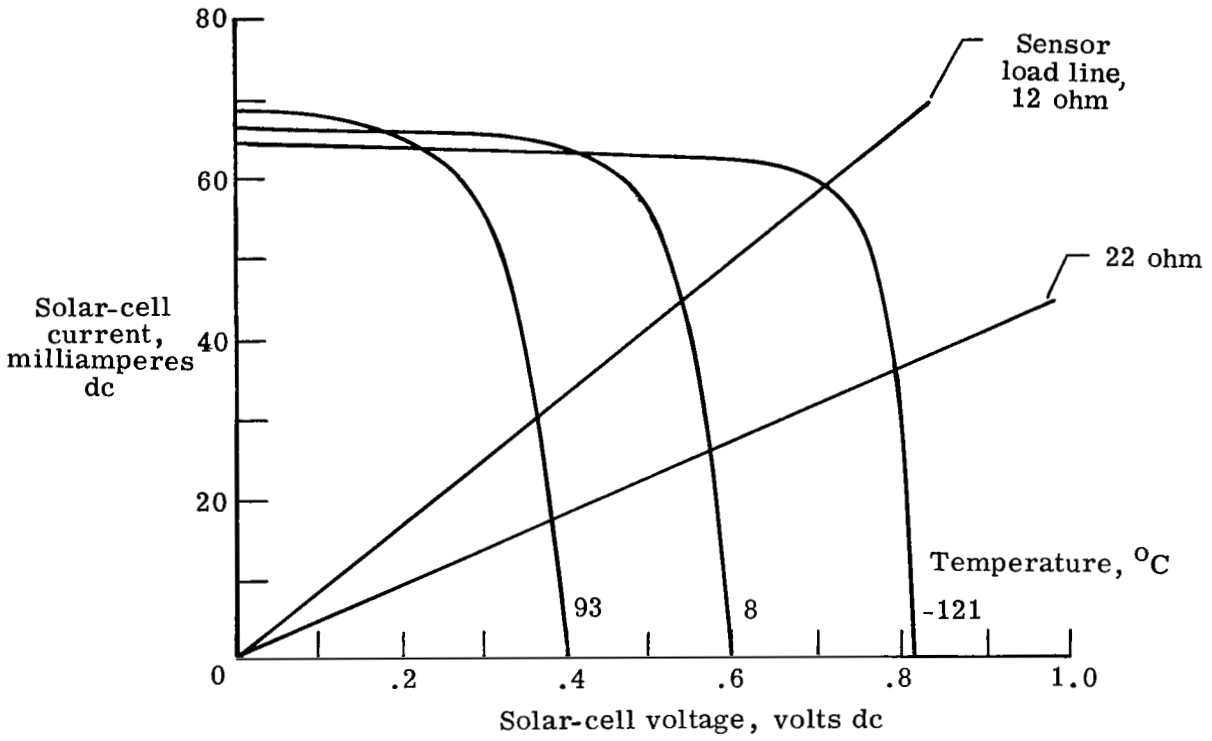

Figure 12.- Sensor characteristics for two load resistance values. Illumination intensity; 140 mW/cm^2; 1- by 2-cm solar cell.

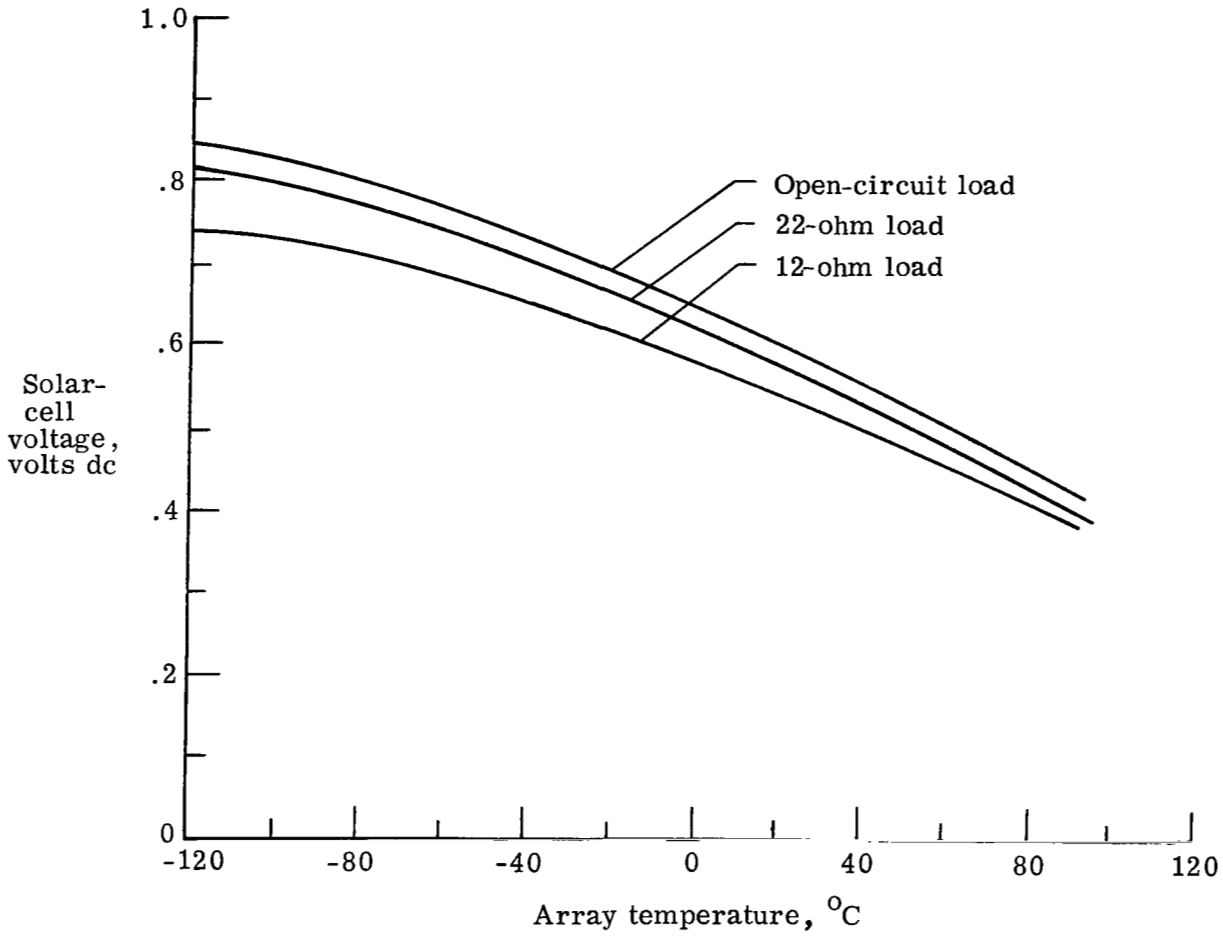

Figure 13.- Variation of sensor voltage with array temperature for various load resistance values. Illumination intensity, 140 mW/cm^2; 1- by 2-cm solar cell.

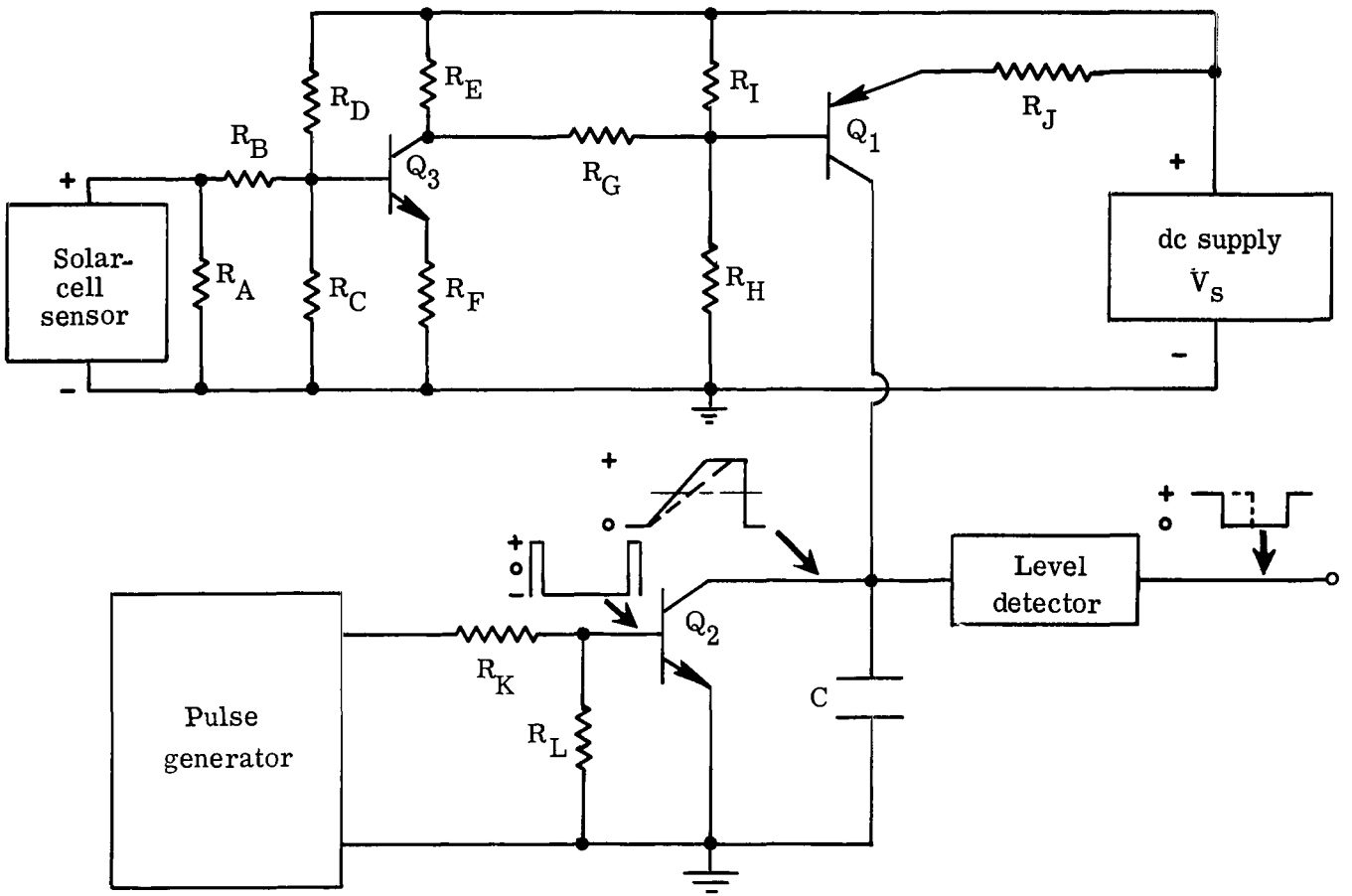

Figure 14.- Control circuit utilizing solar cell as temperature sensor.

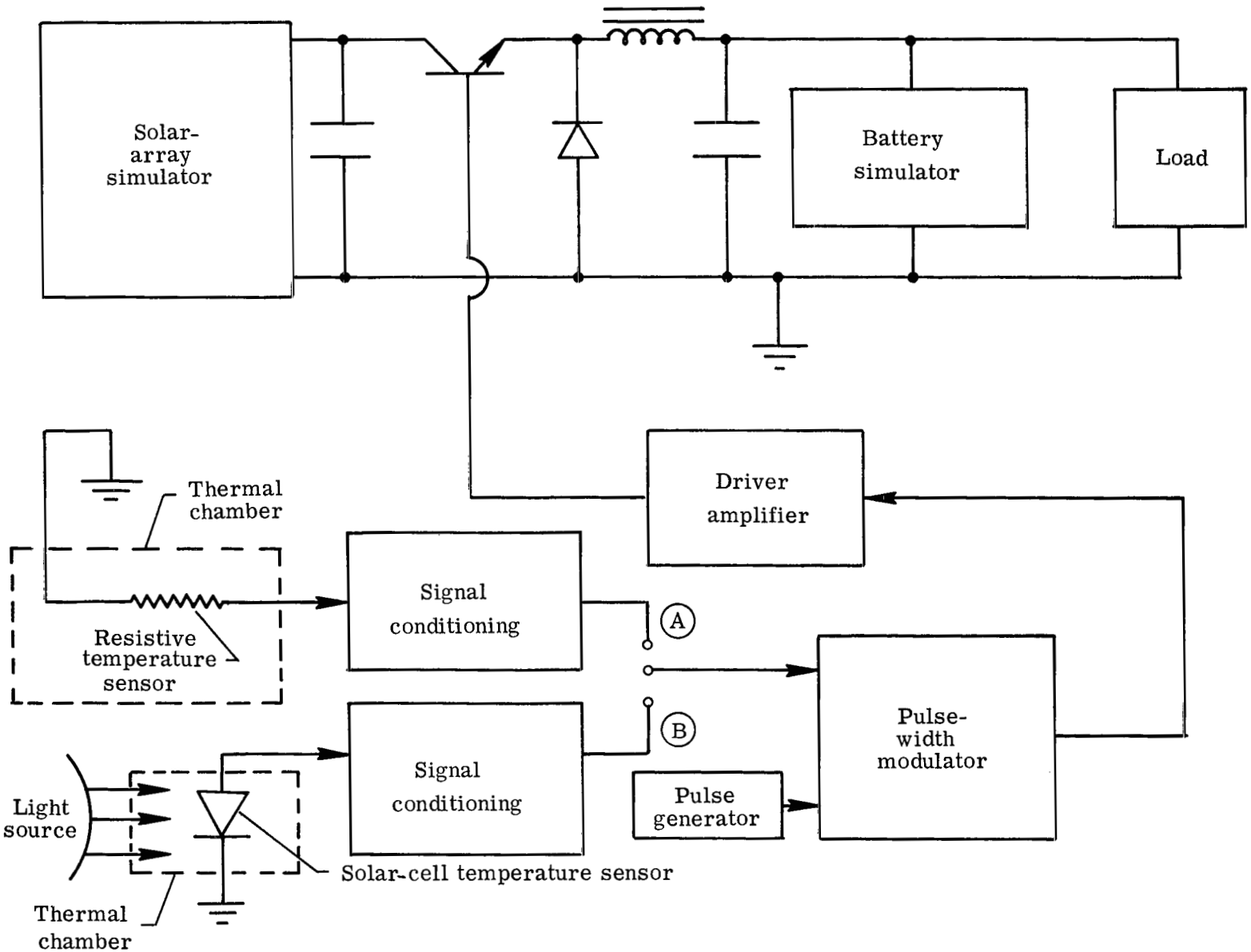

Figure 15.- Performance test setup.

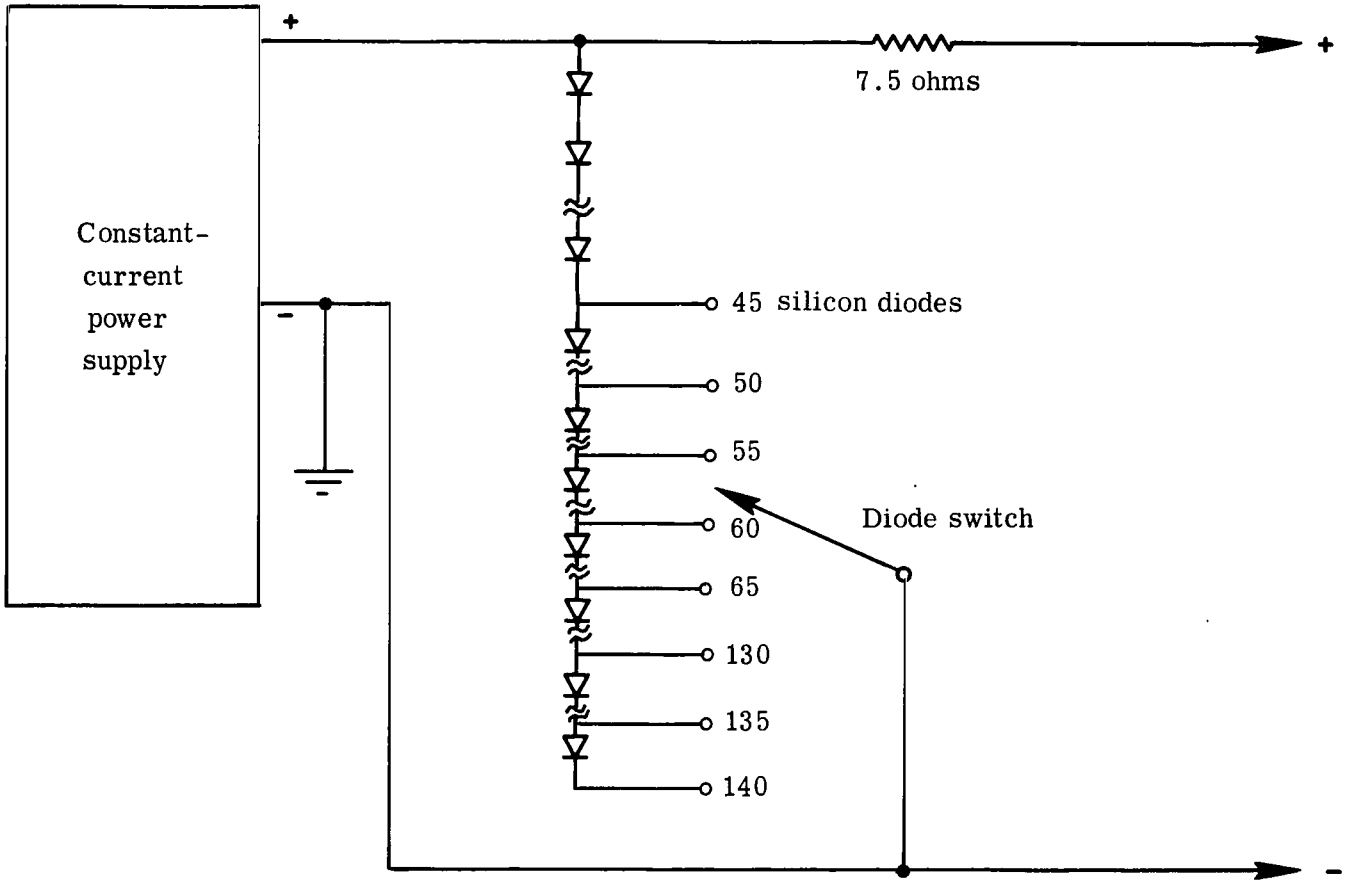

Figure 16.- Solar-cell array simulator.

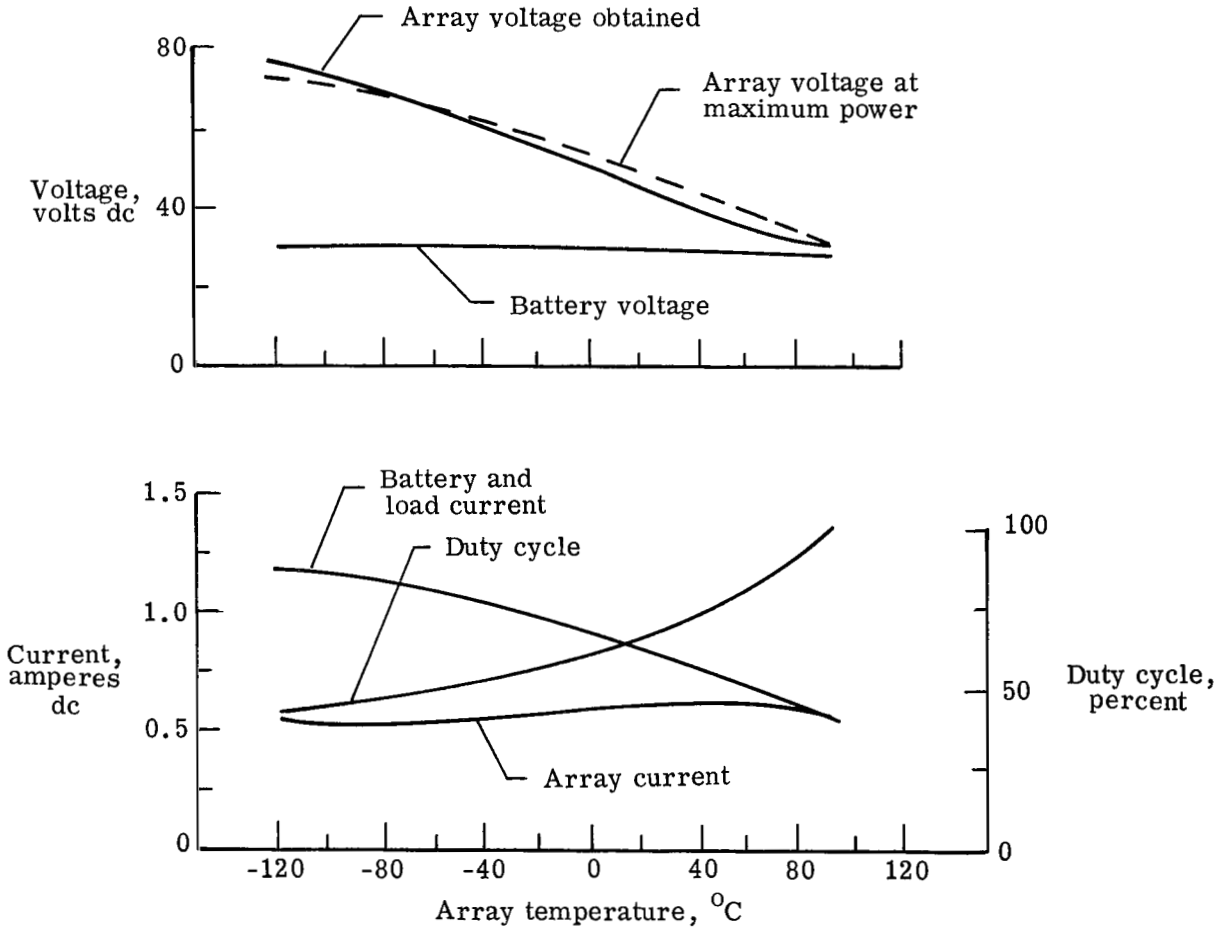

Figure 17.- Power-system performance data.

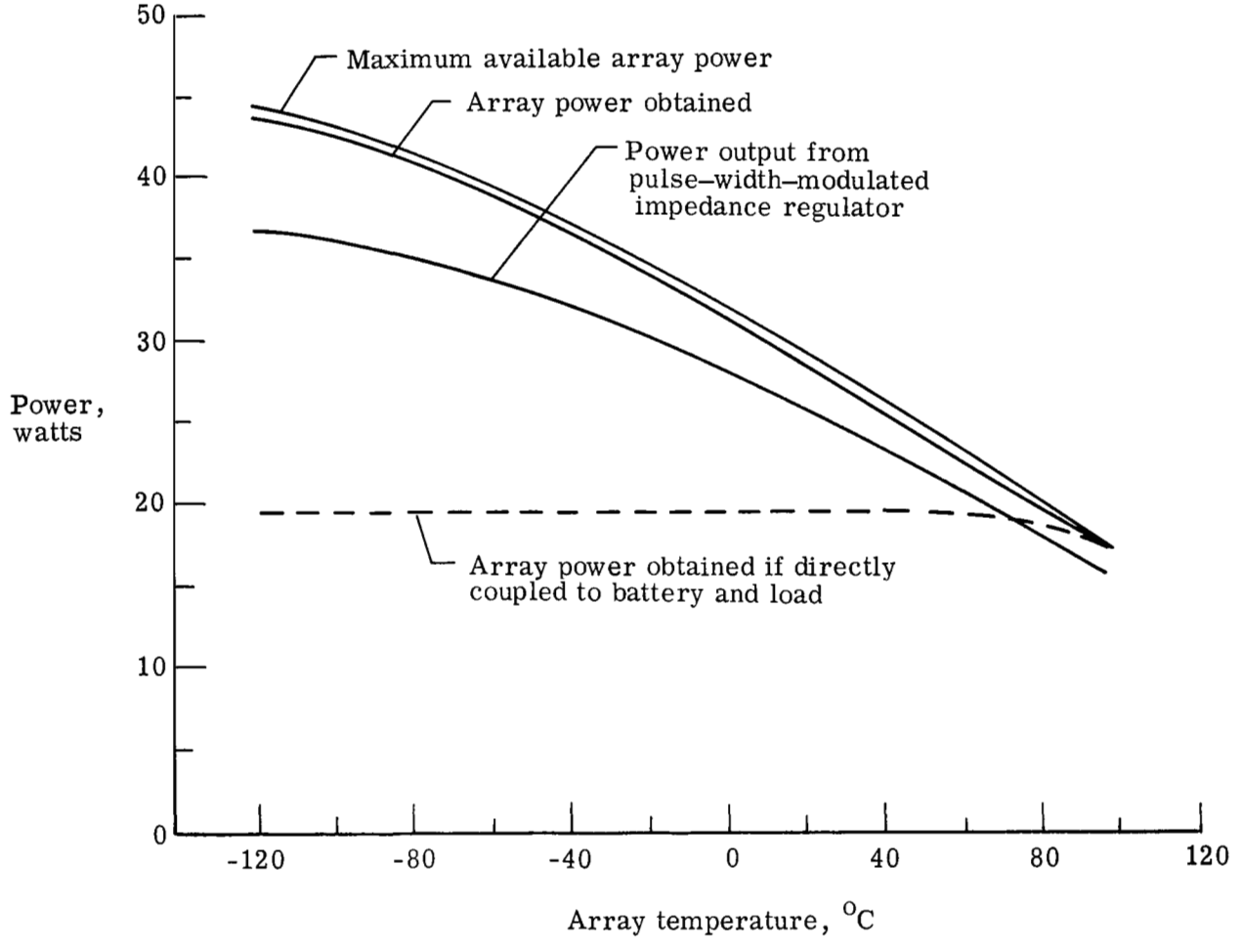

Figure 18.- Comparison between maximum available array power and array power obtained.

"The aeronautical and space activities of the United States shall be conducted so as to contribute . . . to the expansion of human knowledge of phenomena in the atmosphere and space. The Administration shall provide for the widest practicable and appropriate dissemination of information concerning its activities and the results thereof."

— NATIONAL AERONAUTICS AND SPACE ACT OF 1958

NASA SCIENTIFIC AND TECHNICAL PUBLICATIONS

TECHNICAL REPORTS: Scientific and technical information considered important, complete, and a lasting contribution to existing knowledge.

TECHNICAL NOTES: Information less broad in scope but nevertheless of importance as a contribution to existing knowledge.

TECHNICAL MEMORANDUMS: Information receiving limited distribution because of preliminary data, security classification, or other reasons.

CONTRACTOR REPORTS: Scientific and technical information generated under a NASA contract or grant and considered an important contribution to existing knowledge.

TECHNICAL TRANSLATIONS: Information published in a foreign language considered to merit NASA distribution in English.

SPECIAL PUBLICATIONS: Information derived from or of value to NASA activities. Publications include conference proceedings, monographs, data compilations, handbooks, sourcebooks, and special bibliographies.

TECHNOLOGY UTILIZATION PUBLICATIONS: Information on technology used by NASA that may be of particular interest in commercial and other non-aerospace applications. Publications include Tech Briefs, Technology Utilization Reports and Technology Surveys.

Details on the availability of these publications may be obtained from:

SCIENTIFIC AND TECHNICAL INFORMATION OFFICE

NATIONAL AERONAUTICS AND SPACE ADMINISTRATION

Washington, D.C. 20546